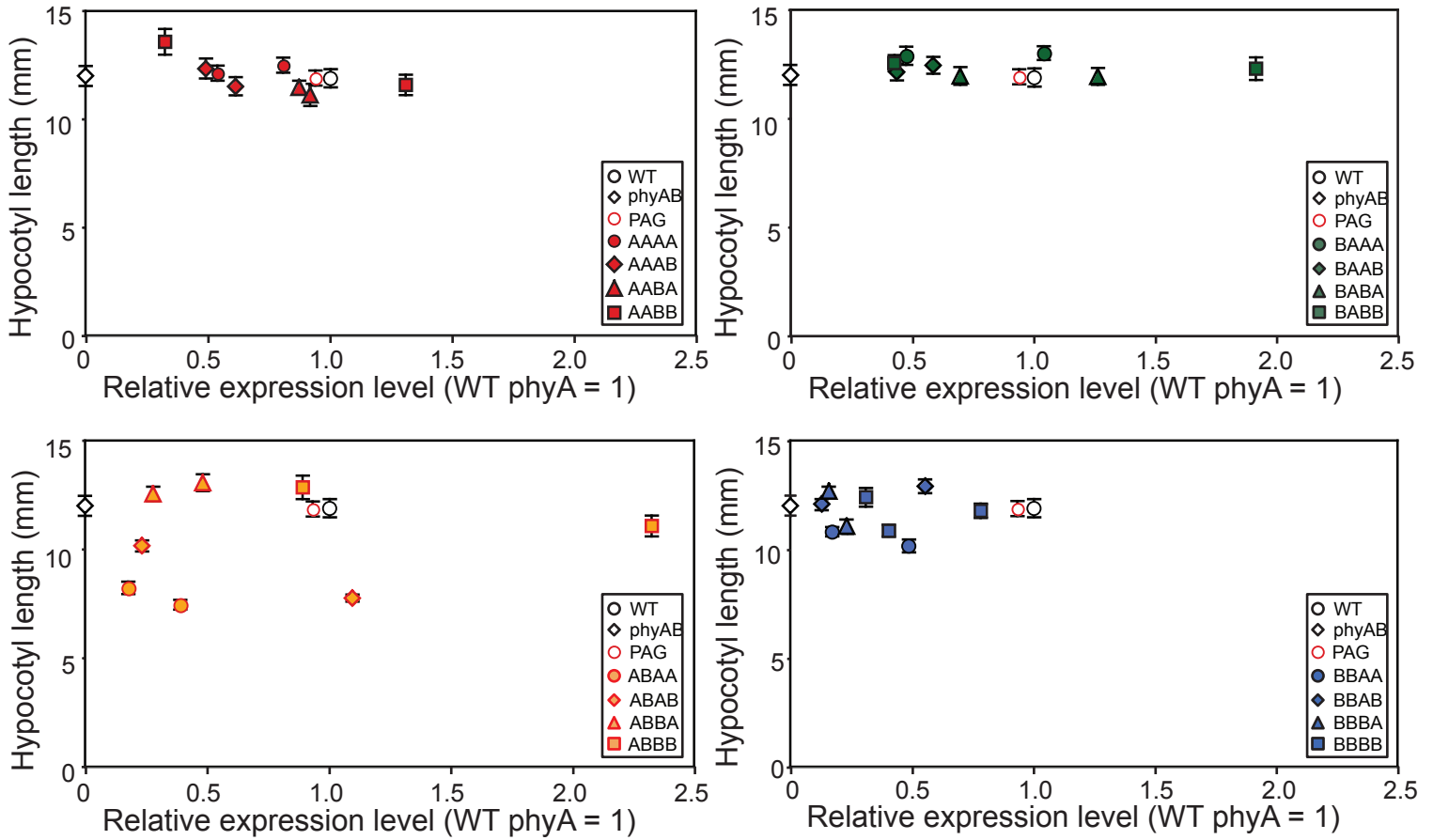


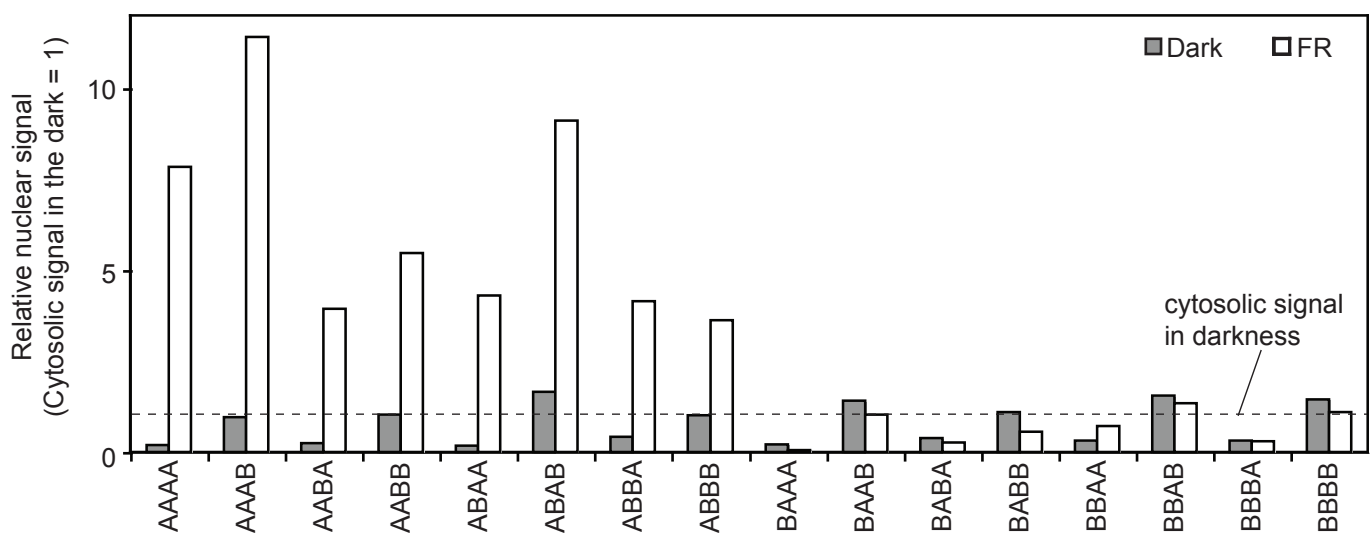
Supplemental Figure 1. Immunoblot detection of endogenous phyA, endogenous phyB, phyA-GFP (PAG and AAAA) and phyB-GFP (PBG and BBBB).

Seedlings were grown for 4 days in the dark. The monoclonal antibodies used to probe the blots are shown on the right. Five micrograms of total protein was loaded in each lane. Anti-phyA and phyB antibodies were raised against the C-terminal moiety of phytochrome (Shinomura et al., 1996). Together with Anti-GFP antibody (Nacalai Tesque, Kyoto, Japan), these antibodies were used to compare the expression levels of chimeric phytochromes. (A) Dilution series analysis of phyB-GFP expression in PBG18, in which phyB-GFP is expressed in the phyB mutant background (Matsushita et al., 2003). Apparent signal intensities are indicated at the bottom, from which a standard curve was obtained. Consequently, the expression level in PBG18 was estimated to be 11.2 (endogenous phyB = 1). (B) Dilution series analysis of phyA-GFP expression in PAG, in which phyA-GFP is expressed in the phyA mutant background (Toledo-Ortiz et al., 2010). The relative expression levels of phyA-GFP in lines, PAG and AAAA 10-4, were estimated to be 0.92 and 0.79 (endogenous phyA = 1), respectively. (C) Dilution series analysis of PAG and PBG 18. The relative amount of phyB-GFP in PBG18 was estimated to be 0.42 (the amount of PAG = 1). (D) Detection of phyA and phyB in control lines (PAG, AAAA 10-4, PBG 18 and BBBB 3-4) with various antibodies.



Supplemental Figure 2. The relationship between hypocotyl length in the dark (ordinate) and protein expression levels (abscissa) in independent transgenic lines.

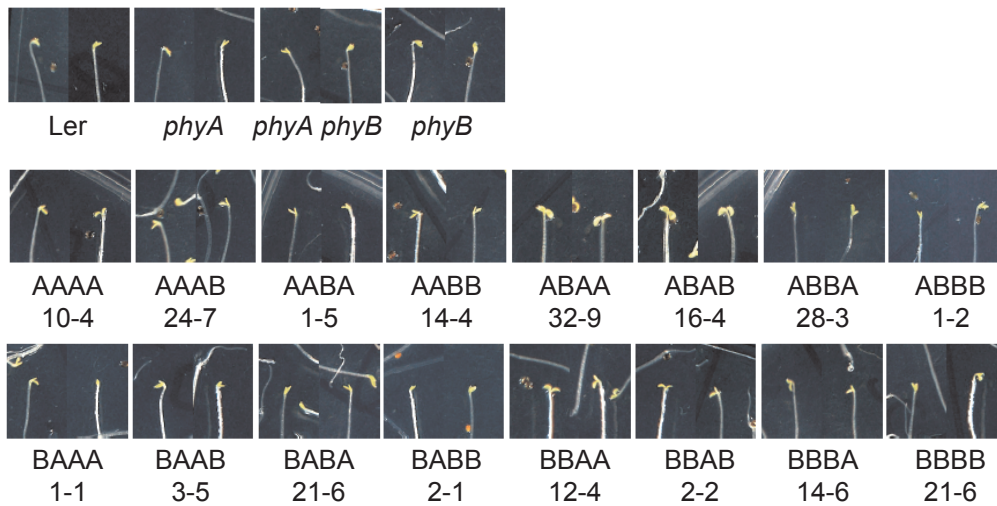
Data are the means \pm SE (n = 25).



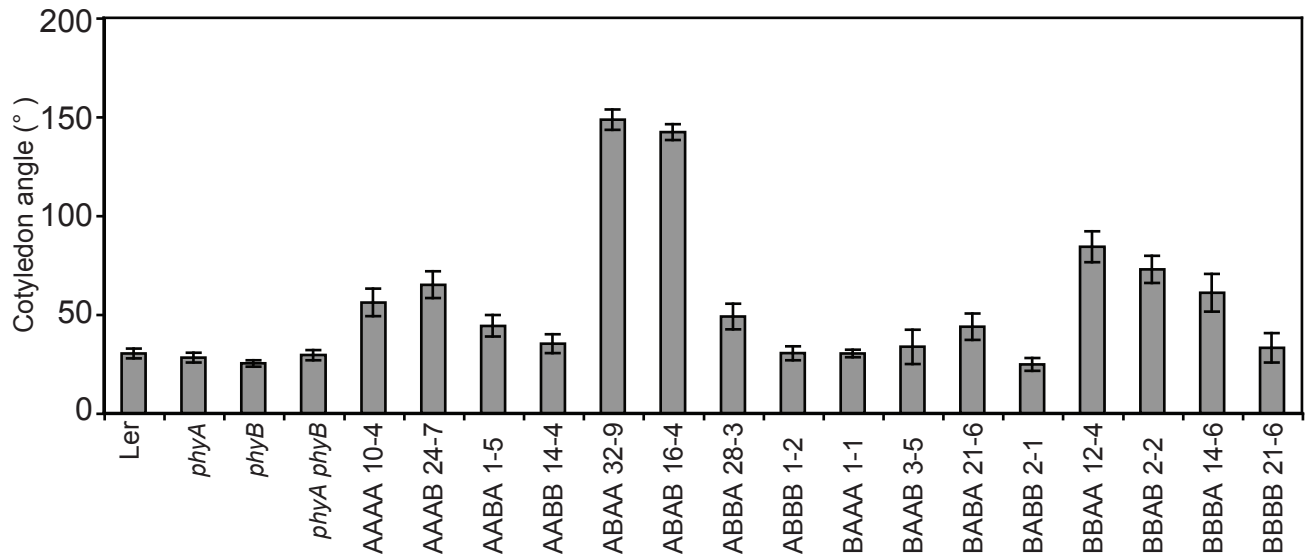
Supplemental Figure 3. Nuclear accumulation of chimeric phytochromes under cFR.

Seedlings were grown in the dark for 5 days. GFP fluorescence intensity in the nucleus was quantified using NIH Image J software as described in Toledo-Ortiz et al., 2010. Data are presented relative to the cytosolic signal in the dark.

A

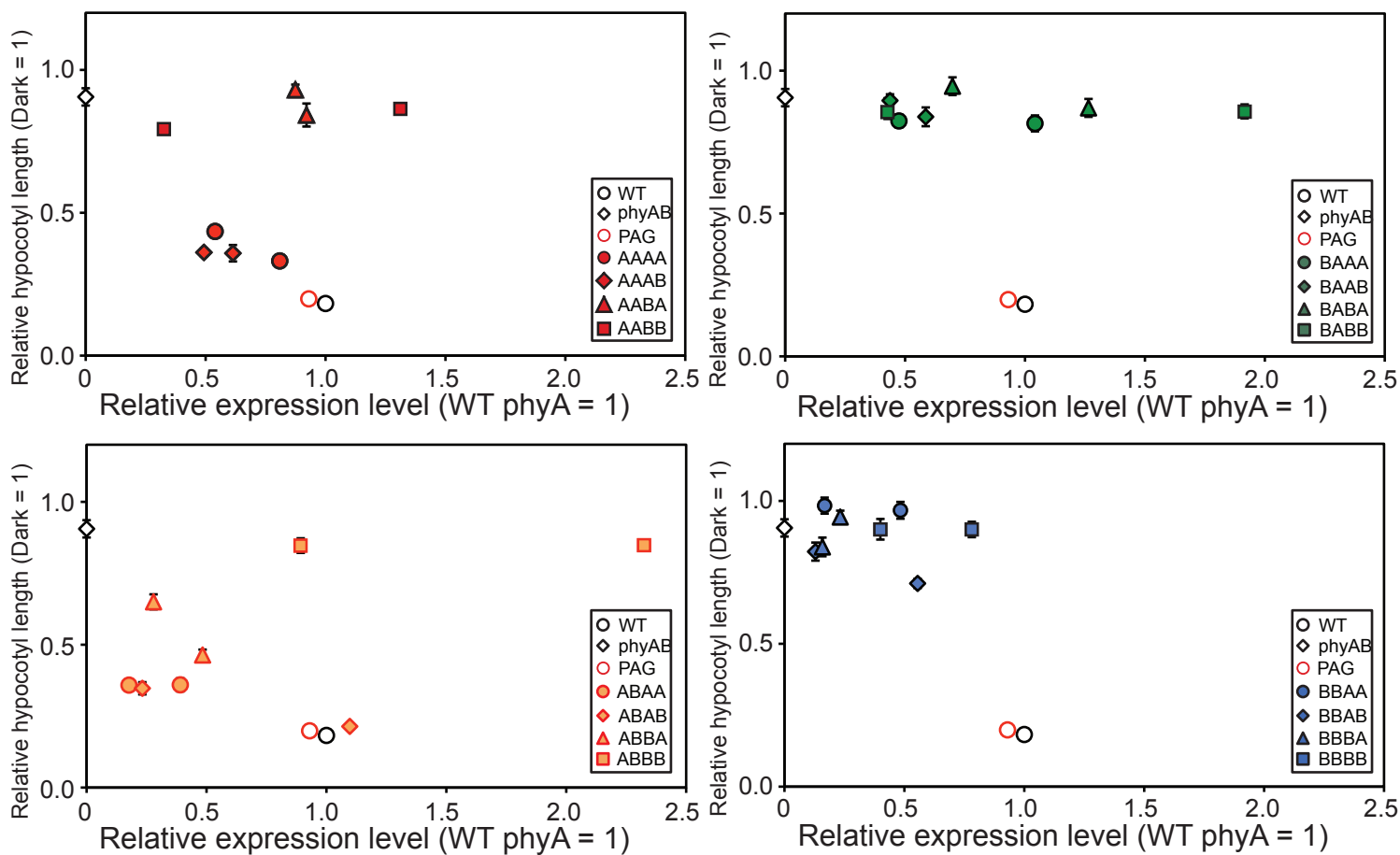


B



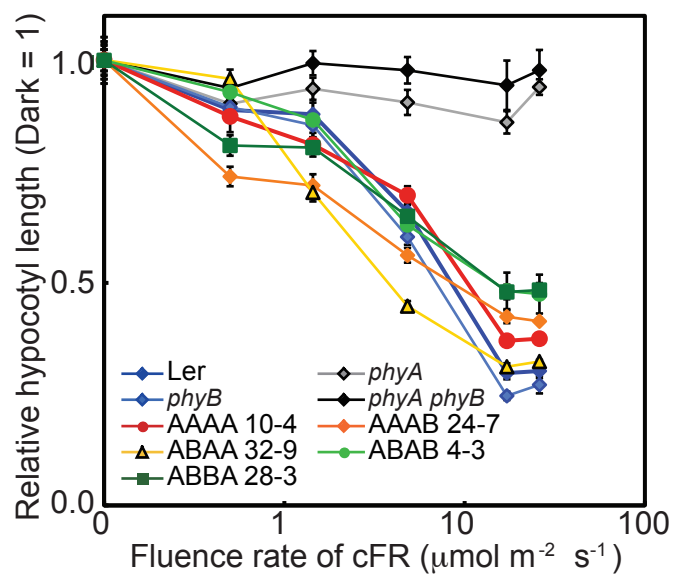
Supplemental Figure 4. Cotyledon-separation in the dark.

(A) Pictures and (B) quantification of the cotyledon-separation angle in the dark. The seedlings were grown in the dark for 5 days. Data are the means \pm SE (n = 25).



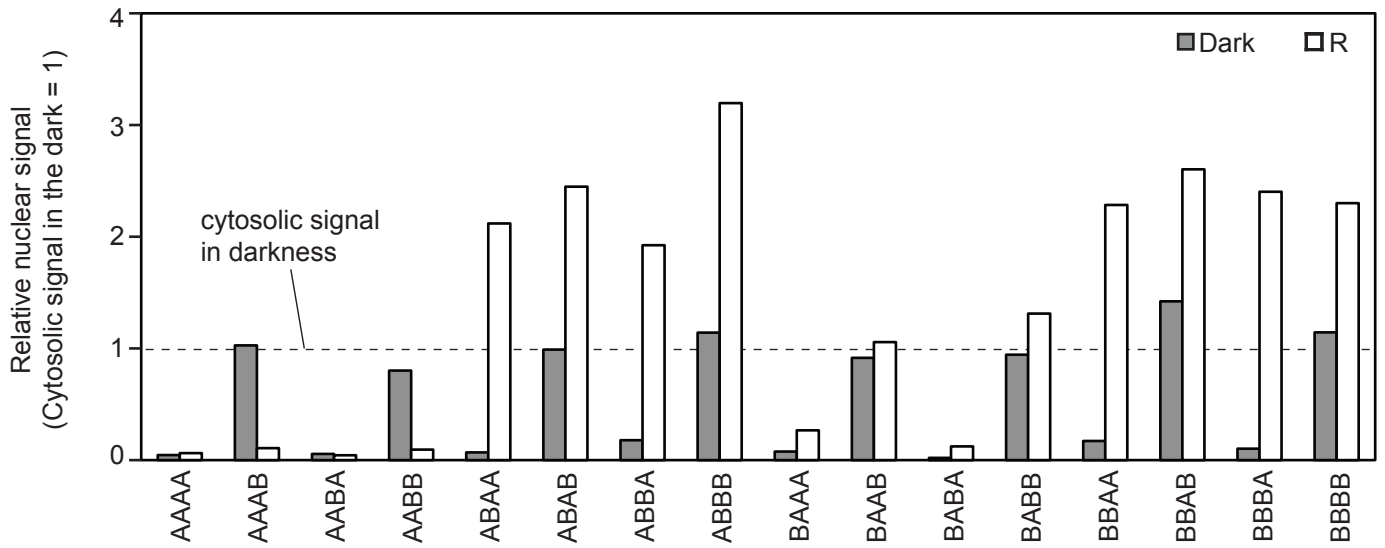
Supplemental Figure 5. The relationship between hypocotyl length under continuous FR (ordinate) and protein expression levels (abscissa) in independent transgenic lines.

Data are the means \pm SE (n = 25).



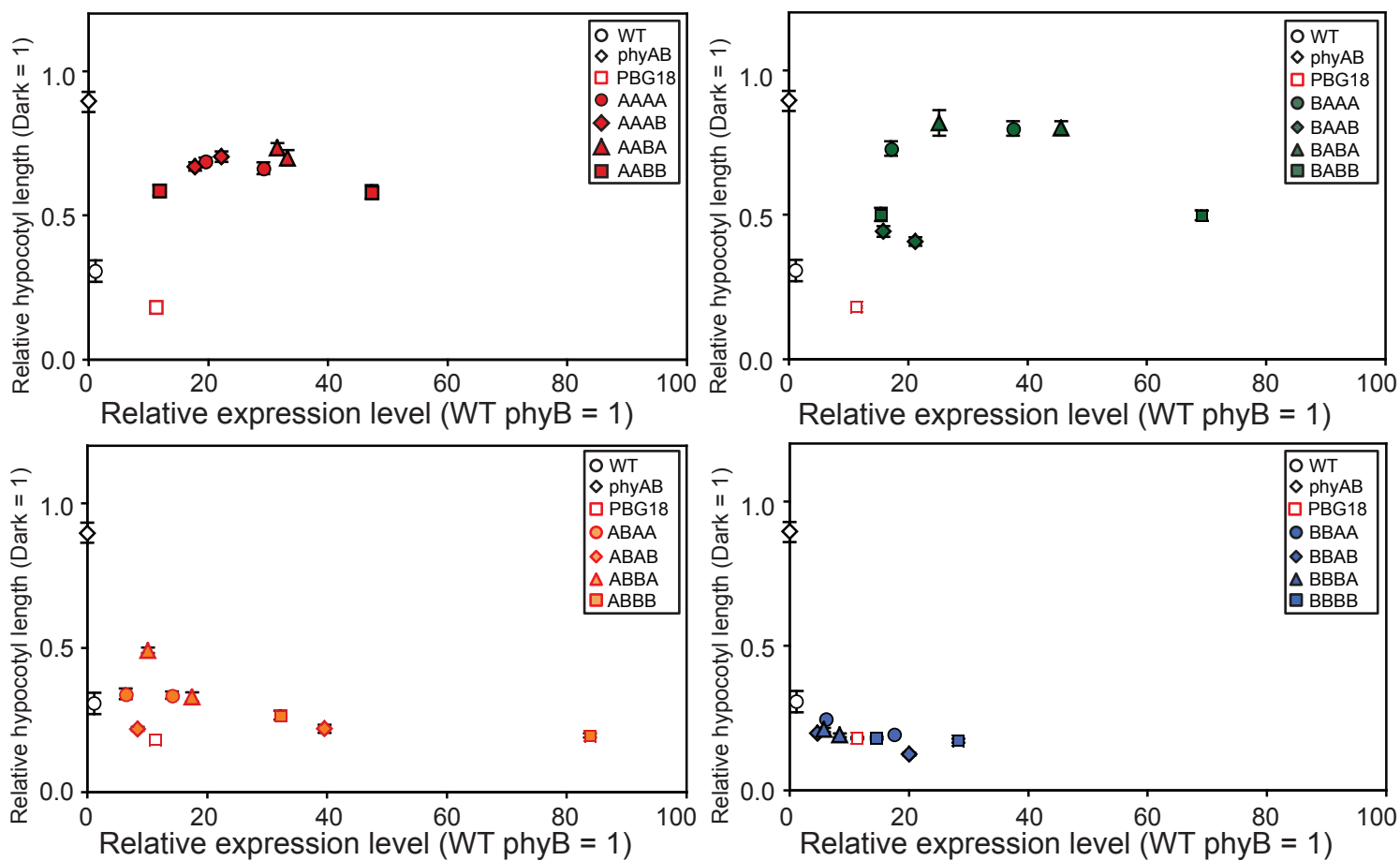
Supplemental Figure 6. Fluence-rate response curves for the inhibition of hypocotyl elongation under cFR.

Seedlings were grown for 5 days under various fluence rates of cFR. Data are the means \pm SE (n = 25).



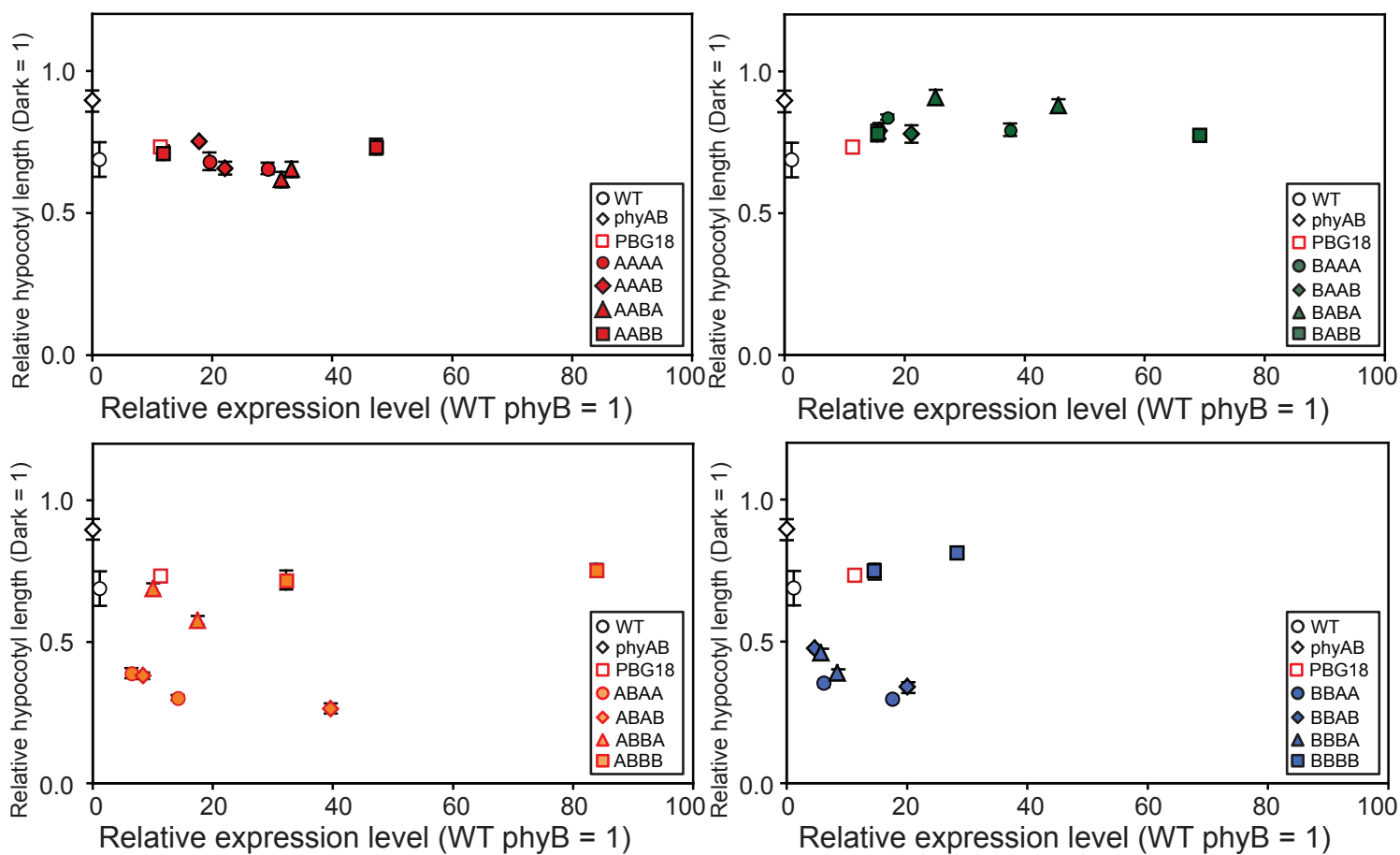
Supplemental Figure 7. Nuclear accumulation of chimeric phytochromes under cR.

Seedlings were grown in the dark for 5 days. GFP fluorescence intensity in the nucleus was quantified using NIH Image J software as described in Toledo-Ortiz et al., 2010. Data are presented relative to the cytosolic signal in the dark



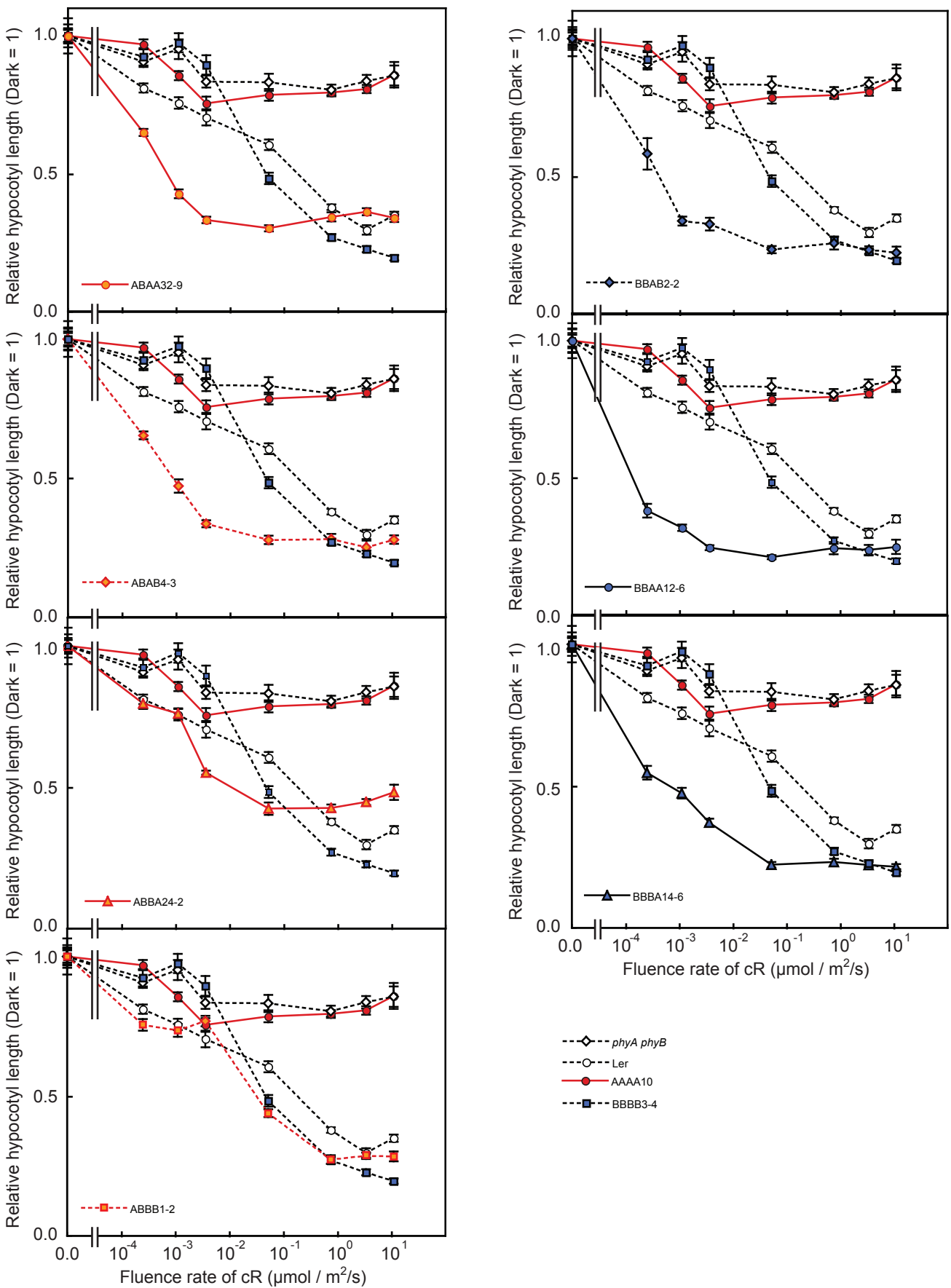
Supplemental Figure 8. The relationship between hypocotyl length under R (ordinate) and protein expression levels (abscissa) in independent transgenic lines.

Data are the means \pm SE (n = 25).



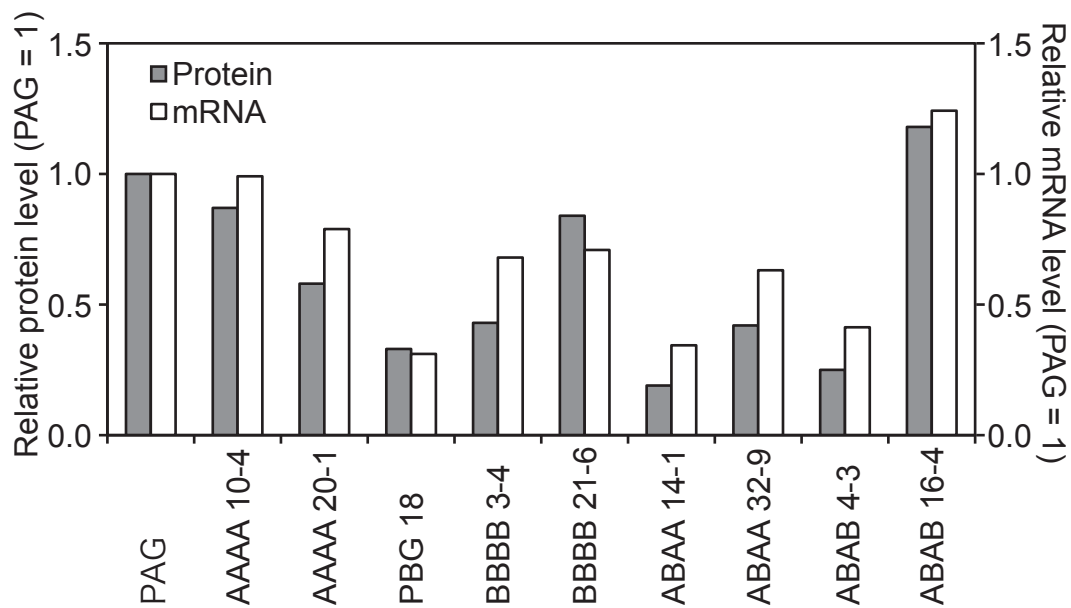
Supplemental Figure 9. The relationship between hypocotyl length under weak R (ordinate) and protein expression levels (abscissa) in independent transgenic lines.

Data are the means \pm SE (n = 25).



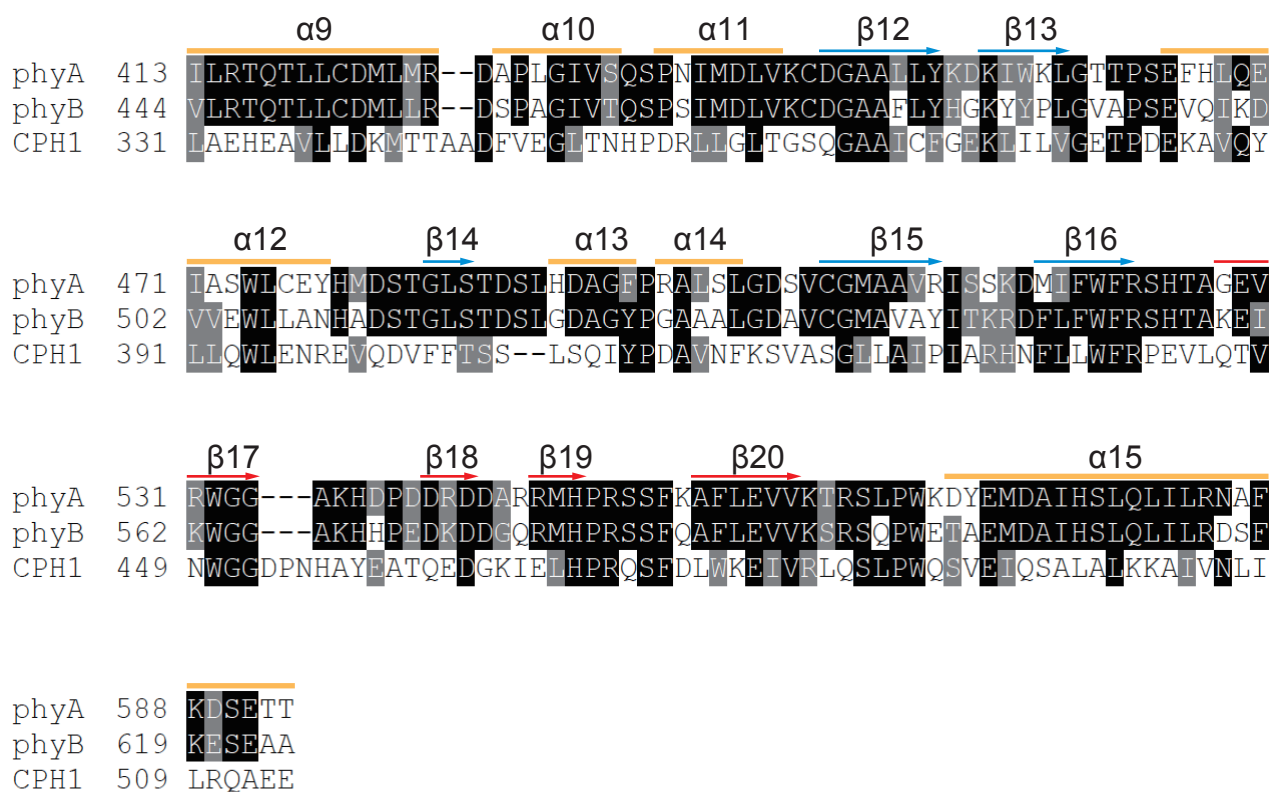
Supplemental Figure 10. Fluence rate response curves for the inhibition of hypocotyl elongation under cR.

Data are the means \pm SE (n = 25).



Supplemental Figure 11. Protein levels of ABAA and ABAB are roughly correlative with those mRNA levels in the dark.

Relative protein and mRNA levels of chimeric phytochromes for the indicated transgenic lines grown in the dark were shown. The protein levels were calculated from the values in Figure 2C. The mRNA levels were determined by Real-time PCR using RNA from 4-day-old seedlings grown in the dark. The data are represented with PAG values set to 1.



Supplemental Figure 12. Alignment of phyA, phyB and bacterial PHY domain sequences.

phyA, *Arabidopsis thaliana* phyA; phyB, *Arabidopsis thaliana* phyB; CPH1, *Synechocystis* PCC6803 Cph1. The PHY domain was delimited as for Figure 1. The β17, β18, β19 and β20 strands (red arrows) form a tongue-like structure. The β-strands and α-helices on the top of the sequences are based on Essen et al., 2008.

Supplemental table 1. Summary of the action of chimeric phytochromes

Construct	Subcellular localization			Degradation in R	Short hypocotyl phenotype			
	Dark ^a	FR ^a	R ^b		Dark	FR	sR ^c	wR ^d
AAAA	N < C	N > C	nd	++	-	+	-	-
AAAB	N = C	N > C	nd	++	-	+ / ++	-	-
AABA	N < C	N > C	nd	++	-	-	-	-
AABB	N = C	N > C	nd	++	-	-	-	-
ABAA	N < C	N > C	NS	+	+	++	++	++
ABAB	N = C	N > C	NS	-	+	++	++	++
ABBA	N < C	N > C	NS	+	-	+	++	+
ABBB	N = C	N > C	NS	-	-	-	++	+
BAAA	N < C	N < C	only in C	-	-	-	-	-
BAAB	N = C	N = C	NS	-	-	-	+	-
BABA	N < C	N < C	only in C	-	-	-	-	-
BABB	N = C	N < C	NS	-	-	-	+	-
BBAA	N < C	N < C	NS	+	-	-	+++	++
BBAB	N = C	N = C	NS	-	-	-	+++	++
BBBA	N < C	N < C	NS	-	-	-	+++	++
BBBB	N = C	N = C	NS	-	-	-	+++	-

^aN and C represent nucleus and cytoplasm, respectively.

^bNS, nuclear speckles; nd, not detected; C, cytoplasm; nd, not detectable.

^cStrong R (10 $\mu\text{mol}/\text{m}^2/\text{s}$)

^dWeak R (0.005 $\mu\text{mol}/\text{m}^2/\text{s}$)